doi:10.1016/j.jmb.2009.09.012 *J. Mol. Biol.* (2009) **xx**, xxx–xxx

JMB

Available online at www.sciencedirect.com

ScienceDirect

ELSEVIER

Relationship between Protein Stabilization and Protein Rigidification Induced by Mannosylglycerate

Tiago M. Pais[1], Pedro Lamosa[1,2], Bertrand Garcia-Moreno[3], David L. Turner[1,4] and Helena Santos[1]*

[1]*Instituto de Tecnologia Química e Biológica, Universidade Nova de Lisboa, Rua da Quinta Grande 6, Apartado 127, 2780-156 Oeiras, Portugal*

[2]*Centro de Ressonância Magnética António Xavier, Instituto de Tecnologia Química e Biológica, Universidade Nova de Lisboa, Avenida da República EAN, Apartado 127, 2781-901 Oeiras, Portugal*

[3]*Department of Biophysics, Johns Hopkins University, 3400 North Charles Street, Baltimore, MD 21218, USA*

[4]*School of Chemistry, University of Southampton, Southampton SO17 1BJ, UK*

Received 15 May 2009; received in revised form 20 July 2009; accepted 6 September 2009

Understanding protein stabilization by small organic compounds is a topic of great practical importance. The effect of mannosylglycerate, a charged compatible solute typical of thermophilic microorganisms, on a variant of staphylococcal nuclease was investigated using several NMR spectroscopy methods. No structural changes were apparent from the chemical shifts of amide protons. Measurements of ^{15}N relaxation and model-free analysis, water–amide saturation transfer (phase-modulated CLEAN chemical exchange), and hydrogen/deuterium exchange rates provided a detailed picture of the effects of mannosylglycerate on the backbone dynamics and time-averaged structure of this protein. The widest movements of the protein backbone were significantly constrained in the presence of mannosylglycerate, as indicated by the average 5-fold decrease of the hydrogen/deuterium exchange rates, but the effect on the millisecond timescale was small. At high frequencies, internal motions of staphylococcal nuclease were progressively restricted with increasing concentrations of mannosylglycerate or reduced temperature, while the opposite effect was observed with urea (a destabilizing solute). The order parameters showed a strong correlation with the changes in the T_m values induced by different solutes, determined by differential scanning calorimetry. These data show that mannosylglycerate caused a generalised reduction of backbone motions and demonstrate a correlation between protein stabilization and protein rigidification.

Edited by A. G. Palmer III

Keywords: staphylococcal nuclease; protein stabilization; NMR; dynamics; chemical shift

Introduction

The mechanism underlying protein stabilization by osmolytes is a challenging research topic. In an early attempt to explain the effects of stabilizers or denaturants on proteins, Tanford and Nozaki proposed that the free energy of transfer of a protein molecule (either in the native or denatured state) from water to an osmolyte solution was given by the sum of the transfer free energies of the solvent-exposed parts. The individual transfer free energies were estimated from the solubility of different peptide model compounds in water and in osmolyte solutions.[1–3] Later, Timasheff and co-workers showed that, upon unfolding, stabilizing compounds were preferentially excluded from the vicinity of the protein, while denaturing agents were

*Corresponding author. E-mail address: santos@itqb.unl.pt.

Abbreviations used: NOE, nuclear Overhauser enhancement; HSQC, heteronuclear single quantum coherence; DSC, differential scanning calorimetry; CLEANEX-PM, CLEAN chemical exchange-phase modulated.

Please cite this article as: Pais, T. M., *et al.*, Relationship between Protein Stabilization and Protein Rigidification Induced by Mannosylglycerate, *J. Mol. Biol.* (2009), doi:10.1016/j.jmb.2009.09.012

preferentially bound.[4–6] The protecting effect would then arise from the larger destabilization of the denatured state over the native state. More recently, Bolen and co-workers have established the validity of the transfer free energy model and concluded that the unfavourable interaction of osmolytes with the protein backbone is the major driving force in protein stabilization.[7–9] Yet, despite the significant progress in this area, the molecular mechanism underlying the osmolyte–protein stabilizing interactions remains elusive. Moreover, the relationship between protein stability and dynamics remains obscure.

The terms "osmolytes" and "compatible solutes" have been used indiscriminately in the literature to designate low molecular mass compounds, either organic or inorganic, that accumulate inside the cell to counterbalance the osmotic pressure of the external medium. However, it has been shown in recent years that the role of these compounds goes beyond osmoprotection. They are involved in the cell response to other types of stress, such as heat or free radicals.[10] Therefore, throughout this work, the terms "compatible solute" or the short form "solute" will be used to discourage the exclusive association of these protecting compounds with osmotic stress.

With the discovery of hyperthermophiles in the early 1980s, it became apparent that organisms adapted to hot environments accumulate compatible solutes that are rarely or never found in mesophiles: these organic molecules typically comprise a free carboxyl group or are phosphodiester compounds; hence, they are negatively charged, contrasting with the zero net charge of solutes typically found in mesophiles. Comparative studies on the performance of different solutes have emphasised the superior ability of negatively charged solutes to increase the protein melting temperature (T_m). For example, glycerol and trehalose increased the T_m of staphylococcal nuclease (SNase) by 0.8 and 12 °C/M, respectively, while mannosylglycerate and mannosyl-lactate induced increments of 17 and 22 °C/M on the same protein.[11] However, our attempts to rationalise the relative magnitudes of the stabilization induced by structurally related solutes on different enzymes were largely frustrated. Even more surprisingly, the degree of stabilization rendered by a particular solute on a series of single mutant proteins varied significantly.[12] These results are difficult to explain with any of the models proposed for the stabilization of proteins by solutes. Putative specific interactions with the surface of the native protein might account for the observed effects, but their existence lacks clear evidence.

Numerous factors that can contribute to the intrinsic stability of globular proteins, especially those from hyper/thermophilic organisms, have been put forward.[13] Hydrophobic packing, hydrogen-bond networks, salt bridges, and Coulomb interactions can increase the stability of a protein if properly optimized.[14] Thus, it is possible that the mode of action of stabilizing solutes involves the optimization of at least some of these features. This line of thought leads us to the central question of how solutes can alter such properties.

It is generally accepted that the structures of proteins are not affected significantly by the presence of solutes, and that structural changes probably do not play a major role in stabilization. On the other hand, clear alterations in protein dynamics have been observed by us and by others.[15–17] Therefore, a comprehensive NMR study of the changes induced by solutes was performed to address the following questions. Is there a correlation between stabilization by solutes and rigidification of the protein? Is this rigidification a global event or is it selective for specific regions of the protein? Is stabilization associated with motional restrictions at specific dynamic regimes?

Protein dynamics consists of a wide range of motions, from small vibrational fluctuations of bond lengths (picosecond to nanosecond timescale) to translations of atom groups (microsecond to millisecond time frame) to concerted motions of whole structural elements (second to minute timescale). For this reason, it is important to access a wide range of motions and timescales to characterise protein dynamics. We used NMR spectroscopy and performed spin relaxation measurements to study fast protein motions at the picosecond to nanosecond timescale, magnetization transfer experiments [with the CLEAN chemical exchange-phase modulated (CLEANEX-PM) sequence] to assess exchange on the millisecond timescale, and conventional proton/deuterium amide exchange measurements to probe events in the minute time frame. The stabilizing solute mannosylglycerate (potassium form) typical of hyperthermophilic organisms and a hyperstable variant of SNase with three amino acid substitutions (P117G, H124L, and S128A) were selected as the model system for this work. KCl and glycerol were used as controls for ionic strength and viscosity, respectively. Changes in protein dynamics were correlated with changes in the melting temperature of the model protein as determined by calorimetric measurements.

Results

Differential scanning calorimetry

The unfolding transition temperatures (T_m) of SNase determined in the presence of urea, glycerol, KCl, and mannosylglycerate are shown in Table 1. Glycerol and KCl were used to assess the contributions of viscosity and ionic strength, respectively; the viscosity of 0.6 M glycerol is identical with that of 0.25 M mannosylglycerate. In the absence of solutes, the T_m was 67.4 °C. Mannosylglycerate increased the T_m in a concentration-dependent manner. On the other hand, 0.6 M glycerol and 0.25 M KCl had little effect, and 0.25 M urea decreased the T_m by 1.6 °C. Furthermore, the presence of

Please cite this article as: Pais, T. M., *et al.*, Relationship between Protein Stabilization and Protein Rigidification Induced by Mannosylglycerate, *J. Mol. Biol.* (2009), doi:10.1016/j.jmb.2009.09.012

Table 1. Transition temperatures for the unfolding of SNase obtained by DSC

	Conc (M)	T_m (°C)	ΔT_m[a] (°C)
No solute	0	67.40±0.41	0
Urea	0.25	65.80±0.23	−1.60
KCl	0.25	66.64±0.10	−0.76
Glycerol	0.60	67.21±0.22	−0.19
Mannosylglycerate	0.15	69.15±0.29	+1.75
	0.25	70.58±0.11	+3.18
	0.35	72.00±0.15	+4.60
	0.50	74.28±0.20	+6.88

[a] Difference of SNase T_m value in the presence and in the absence of different solutes.

mannosylglycerate did not affect the extent of reversibility of the protein unfolding reaction.

Relaxation data

Transverse relaxation rates (R_2) were determined as a function of protein concentration using samples with 0.5, 1.0, 1.5, 2.5, and 3.5 mM of SNase in the presence of 0.35 M mannosylglycerate to test for possible protein aggregation (not shown). These results show that there is no significant concentration dependence of R_2 below 3.5 mM, and a protein concentration of 2.6 mM was used for the remaining experiments.

Longitudinal (R_1) and transverse relaxation rates as well as heteronuclear nuclear Overhauser enhancement (h-NOE) values were obtained at the different experimental conditions for a total of 93 backbone amide groups, accounting for 80% of the backbone NHs previously assigned.[18,19] The average relaxation rates and h-NOE values measured in the control conditions (absence of solutes) are in general agreement with those obtained for another SNase variant (H124L).[20]

With few exceptions, the calculated R_2/R_1 ratios were very homogeneous for the protein backbone in each of the conditions tested (Fig. 1). The total correlation time (τ_c) of the protein was estimated from the average R_2/R_1 ratio, excluding values that fail the selection criteria described by Tjandra *et al.*[21] This correlation time showed a positive dependence on mannosylglycerate concentration, while the opposite effect was observed with KCl and urea, which appears to be in fair agreement with the variation of the viscosity of the solution. However, bulk viscosity was not solely responsible for the estimated total correlation time, since glycerol (0.6 M) gave rise to a τ_c of 8.4 ns, while mannosylglycerate, at the same bulk viscosity (0.25 M), gave rise to a τ_c of 10.4 ns (Table 2). In the absence of solutes, an increase in the experimental temperature caused a decrease in the total correlation time. The h-NOE values showed no apparent trend as a function of mannosylglycerate concentration.

Diffusion tensor

The diffusion tensor and all subsequent parameters of the internal dynamics were obtained from the experimental data using the crystal structure of the PHS variant of SNase (PDB entry code: 1EY8) as a structural model (Fig. 2). This structure is markedly asymmetric, as shown by the principal components of the inertial tensor ($I_{xx}/I_{yy}/I_{zz}$=1.00:0.94:0.71). The rotational diffusion tensor of the SNase was fitted for each examined condition using relaxation data from 38 residues that passed the selection criteria outlined by Tjandra *et al.*[21] in all cases. The statistical analysis routine embedded in the program Tensor2[22,24] was used to test models for the diffusion tensor of the protein; the *F*-test showed that the fully anisotropic model gave a statistically significant improvement over the isotropic or the axially symmetric models in each case (Fexp>0.1, *F*-test). The data presented in Table 2 characterise the diffusion tensor of the protein for all tested conditions.

The orientation of the diffusion tensor relative to the inertial tensor did not change significantly in the presence of the four examined solutes or with temperature. The diffusion rates (D_x, D_y, and D_z)

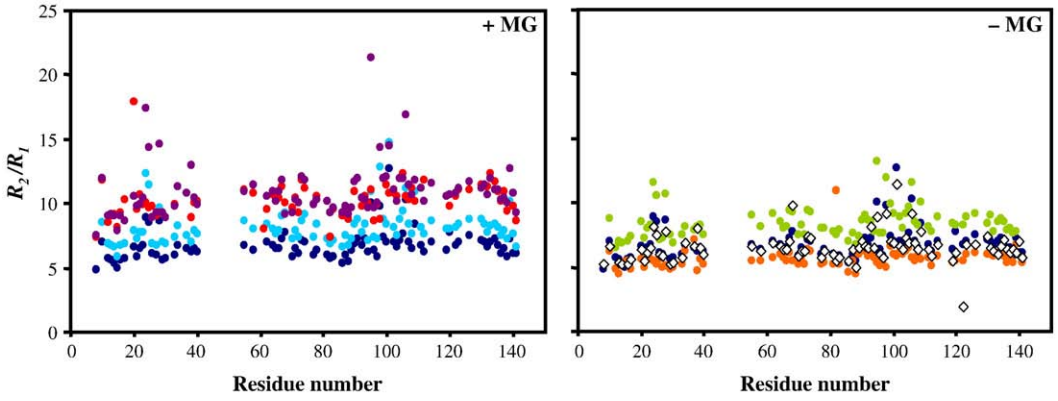

Fig. 1. Effect of mannosylglycerate and other solutes on the R_2/R_1 ratio of each amide group. Left, variation of R_2/R_1 ratios as a function of mannosylglycerate concentration: 0 M (dark blue circles), 0.15 M (light blue circles), 0.25 M (red circles), and 0.35 M (purple circles). Right, R_2/R_1 ratio of amide groups in the absence (dark blue circles) and in the presence of 0.25 M KCl (orange circles), 0.25 M urea (open diamonds), and 0.60 M glycerol (green circles). MG, mannosylglycerate.

Please cite this article as: Pais, T. M., *et al.*, Relationship between Protein Stabilization and Protein Rigidification Induced by Mannosylglycerate, *J. Mol. Biol.* (2009), doi:10.1016/j.jmb.2009.09.012

Table 2. Characterisation of the diffusion tensor obtained for SNase at different experimental conditions, using the Tensor2 program[22]

	32 °C	37 °C						42 °C
	No solute	Urea, 0.25 M	No solute	KCl, 0.25 M	Glycerol, 0.60 M	MG, 0.15 M	MG, 0.25 M	MG, 0.35 M	No solute
τ_c (ns)[a]	8.6 (±1.1)	6.5 (±1.0)	6.8 (±1.2)	5.6 (±1.0)	8.4 (±1.3)	8.7 (±1.8)	10.4 (±1.8)	10.3 (±1.5)	6.2 (±1.2)
α (deg)[b,c]	−84.9 (±14.1)	−76.2 (±8.1)	−70.9 (±7.9)	−78.9 (±10.2)	−66.9 (±6.5)	−61.5 (±14.9)	−72.3 (±7.9)	−52.1 (±8.5)	−67.0 (±12.2)
β (deg)	−64.6 (±3.3)	−65.6 (±1.6)	−64.7 (±1.5)	−64.0 (±1.8)	−64.6 (±1.7)	−63.8 (±2.0)	−65.4 (±1.5)	−68.6 (±2.7)	−63.5 (±2.0)
γ (deg)	−20.7 (±5.2)	−18.7 (±2.7)	−16.0 (±2.5)	−7.2 (±3.0)	−19.0 (±2.6)	−14.0 (±3.0)	−9.3 (±2.5)	−21.3 (±3.6)	−16.7 (±3.2)
D_x ($\times 10^7$ s^{-1})	1.40 (±0.03)	1.67 (±0.02)	1.65 (±0.02)	1.80 (±0.02)	1.43 (±0.02)	1.46 (±0.02)	1.25 (±0.01)	1.28 (±0.02)	1.75 (±0.03)
D_y ($\times 10^7$ s^{-1})	1.58 (±0.04)	1.86 (±0.02)	1.83 (±0.02)	1.98 (±0.03)	1.61 (±0.02)	1.56 (±0.02)	1.39 (±0.01)	1.44 (±0.02)	1.92 (±0.03)
D_z ($\times 10^7$ s^{-1})	1.90 (±0.03)	2.34 (±0.02)	2.30 (±0.02)	2.48 (±0.03)	1.95 (±0.02)	1.92 (±0.02)	1.68 (±0.01)	1.70 (±0.02)	1.45 (±0.03)

[a] The total correlation time (τ_c) was calculated using the trimmed average of R_2/R_1 ratios, with errors taken from the SD of the results, according to the procedures outlined by Tjandra *et al.*[21] MG, mannosylglycerate.
[b] α, β, γ, D_x, D_y, and D_z describe the orientation and amplitude of the principal components of the diffusion tensor in the frame of the PDB structure 1EY8.
[c] The errors were estimated on the basis of 600 Monte Carlo simulations using a routine embedded in the Tensor2 program.

were slowed down considerably in the presence of increasing concentrations of mannosylglycerate. The addition of glycerol also caused a reduction in the diffusion rates, but to a lesser extent than that with mannosylglycerate (0.25 M), while KCl and urea had the opposite effect. Not surprisingly, increasing temperatures also gave rise to increasing diffusion rates.

Internal mobility

The internal mobility of each NH vector was characterised by one of five possible models (see Material and Methods) according to the flow chart proposed by Mandel *et al.*[25] In each case, the majority were fitted by the simplest model (Table 3). The addition of glycerol and mannosylglycerate did not appear to change significantly the nature of the mobility of the amide groups. However, KCl induced a considerable simplification of the dynamics (22 extra residues were fitted with the simplest model), mostly due to reduced chemical exchange contributions (models 3 and 4).

The internal mobility of this protein on the picosecond to nanosecond timescale is intrinsically small, with an average S^2 value of 0.896 in the absence of stabilizing solutes at 37 °C; among the residues that were analysed, only Gly50 and Ala69 have S^2 values below 0.80. Still, the presence of mannosylglycerate induced a further restriction on the fast-scale movements of the backbone amides (Fig. 3). The magnitude of this restriction, reflected by the order parameter average, displayed an almost linear correlation with the increase of the melting temperature caused by the addition of mannosylglycerate. This correlation can be generalised by plotting all of the data as a function of $(T_m - T)$, in which T_m is the melting temperature of unfolding as measured by differential scanning calorimetry (DSC) and T is the experimental temperature (Fig. 4). Solutions containing glycerol and KCl, as controls for the effects of viscosity and ionic strength comparable with that of 0.25 M mannosylglycerate, had a much smaller influence on S^2 values than did mannosylglycerate (Fig. 4). Urea, a destabilizing solute, brought about a decrease in the average S^2 values.

There was no obvious correlation between S^2 values of individual residues and residue solvent exposure, side chain, or surface charge. However, secondary structural elements appeared to slightly influence the effect of mannosylglycerate on the mobility of amide bonds (the S^2 values averaged over each secondary structural element of the protein are shown in Fig. 5). Further support for this observation is obtained by analysing the average slope for the S^2 variation as a function of mannosylglycerate concentration: this is 30% larger for the regions of defined secondary structure (0.10 M^{-1}) than for the regions of ill-defined structure (0.07 M^{-1}). The motions of the β-strands appear to be more restricted by the presence of mannosylglycerate than those of α-helices.

Please cite this article as: Pais, T. M., *et al.*, Relationship between Protein Stabilization and Protein Rigidification Induced by Mannosylglycerate, *J. Mol. Biol.* (2009), doi:10.1016/j.jmb.2009.09.012

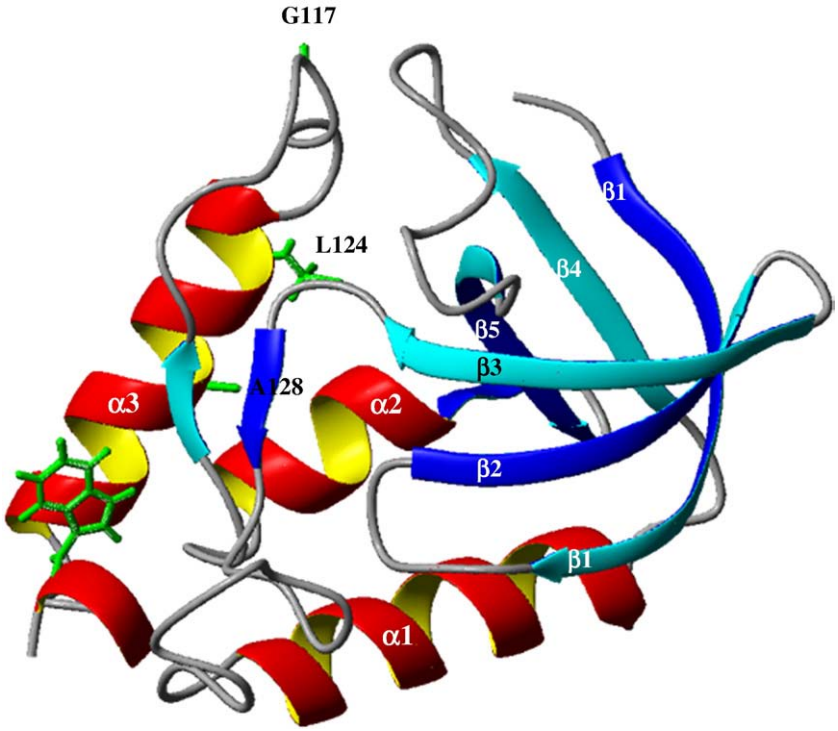

Fig. 2. Ribbon diagram of the PHS variant of SNase. Elements of secondary structure are labelled. Views were generated with MOLMOL[23] using PDB entry 1EY8.

Water–amide proton saturation transfer experiments

In the CLEANEX-PM experiment,[26] the dependence of peak volumes on mixing time (τ_m) is given by the following equation:[27–30]

$$V/V_0 = [k/(R_1a + k - R_1b)] \times \{\exp(-R_1b \times \tau_m) - \exp[-(R_1a + k)\tau_m]\} \quad (1)$$

where k is the normalized rate constant related to the pseudo-first-order forward rate constant $k_{AB}(NH \rightarrow H_2O) = X_B \times k$, with X_B being the molar fraction of water (≈ 1); V the peak volume obtained from the (CLEANEX-PM)–fast heteronuclear single quantum coherence (FHSQC) spectra at a given mixing time, τ_m; and V_0 the reference peak volume obtained with the fast-HSQC spectrum. The R_1a and R_1b parameters refer to the longitudinal relaxation rates of the amide and of the water molecules, respectively. At very short mixing times, Eq. 1 can be approximated by:

$$V/V_0 = k \times \tau_m \quad (2)$$

and the water–amide exchange rates can be calculated from the initial slope of the plot V/V_0 *versus* τ_m. The degree of water saturation in each experiment was determined and used to correct the values obtained from the initial slope analysis[31] simply by dividing k by the fraction of unsaturated water.

In the absence of solutes and at 37 °C, a 35-ms CLEANEX-PM mixing time allowed the observation of 18 assigned resonances: H8, A17, D19, G20, K28, G29, T33, N68, K70, T82, G86, G96, K97, M98, A102,

Table 3. Number of residues assigned to each dynamic model at different experimental conditions

	32 °C	37 °C							42 °C
Model[a]	No solute	Urea, 0.25 M	No solute	KCl, 0.25 M	Glycerol, 0.60 M	MG, 0.15 M	MG, 0.25 M	MG, 0.35 M	No solute
1 (S^2)	72	54	51	73	54	64	58	48	57
2 (S^2, τ_e)	6	4	6	2	2	2	4	5	13
3 (S^2, R_{ex})	9	17	19	10	24	15	10	20	11
4 (S^2, τ_e, R_{ex})	4	3	6	1	1	2	2	3	4
5 (S^2_s, S^2_f, τ_e)	2	13	11	7	9	10	18	16	8
Not fitted	0	2	0	0	1	0	1	1	0

[a] S^2 is the square of the generalised order parameter characterising the amplitude of the internal motions; τ_e is the effective correlation time for the internal motions; R_{ex} is the exchange contribution to T_2; and the subscripts "f" and "s" indicate fast and slow timescales, respectively. MG, mannosylglycerate.

Please cite this article as: Pais, T. M., *et al.*, Relationship between Protein Stabilization and Protein Rigidification Induced by Mannosylglycerate, *J. Mol. Biol.* (2009), doi:10.1016/j.jmb.2009.09.012

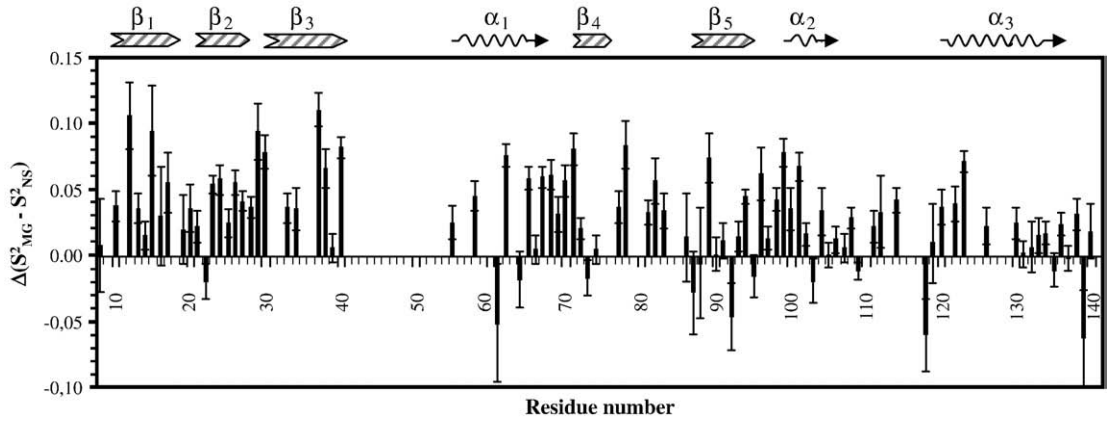

Fig. 3. Changes in the generalised order parameters (S^2) induced by the presence of 0.35 M mannosylglycerate. Subscripts "MG" and "NS" refer to 0.35 M mannosylglycerate and no solute addition, respectively. Elements of secondary structure are also represented.

N119, T120, and Q123. Some of these resonances (D19, G20 N68, K70 T82, G86, A102, and T120) were not detected in the CLEANEX-PM spectra with shorter mixing times, and thus their exchange rates were not calculated. Resonances of L14, G55, and K70 were additionally detected in the presence of KCl, but only with the 35-ms mixing time.

The water–amide proton exchange rates of all accessible resonances, except K97, were lower in the presence of glycerol and mannosylglycerate (Fig. 6). Mannosylglycerate induced a marginally larger reduction of the exchange rates than glycerol. KCl induced only a slight decrease in the magnitude of the exchange rates. On average, mannosylglycerate induced a 1.8-fold decrease in the exchange rates, while glycerol and KCl caused an average reduction of 1.5- and 1.2-fold, respectively. The ratio between exchange rates in the presence and in the absence of solutes was similar for all accessible residues, with an SD of 17% in the case of mannosylglycerate and 12% in the case of glycerol and KCl. There is no clear correlation between these effects and the stability of SNase.

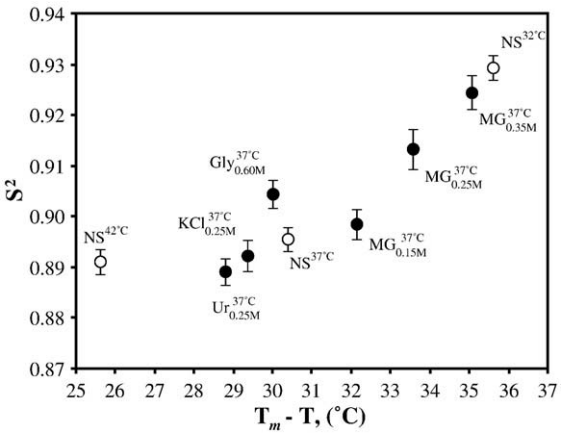

Fig. 4. Plot of the average S^2 values as a function of the shift away from the melting temperature. The $(T_m - T)$ parameter is the difference between the temperature at which relaxation values were measured and the T_m of the protein in the presence of a given solute. NS, no solute; Gly, glycerol; Ur, urea; MG, mannosylglycerate. The subscripts give the concentration of the solute (M) and the superscripts are the experimental temperatures (°C). The errors bars represent the error of the average calculated from the individual S^2 uncertainties.

Hydrogen/deuterium exchange rates

The amide protons of the PHS variant of SNase exchange with deuterium from the solvent at widely different rates, from milliseconds to several hours. Amide protons with lifetimes shorter than the experimental dead time of 25 min could not be observed by this method. In the presence of KCl (0.25 M) at 37 °C, the exchange rates of 66 amide protons could be determined (Fig. 7); 22 other amides were detected only in the first spectrum, having lifetimes close to the dead time, and one other, V99, exchanged extremely slowly. With mannosylglycerate, five extra resonances were detected in the first spectrum but the rates of exchange were too fast to be measured. The hydrogen/deuterium exchange rates displayed a general decrease in samples containing mannosylglycerate, with a maximum 38-fold for V66 at 37 °C. In the presence of glycerol (viscosity control), a decrease of the exchange rates (as compared to KCl) was also observed, but it was much smaller than with mannosylglycerate. Solute-induced changes showed no obvious correlation with properties such as accessible molecular surface, residue charge, or hydrophobicity. Nevertheless, a slight trend was observed with the effect of mannosylglycerate being more pronounced for the most protected amide protons (Supplementary Fig. S1).

According to the scheme shown in Eq. 3, the hydrogen exchange rates can provide information on the thermodynamics of the structural opening reaction that allows the hydrogen/deuterium exchange.[32] In stable folded proteins, the so-called

Please cite this article as: Pais, T. M., *et al.*, Relationship between Protein Stabilization and Protein Rigidification Induced by Mannosylglycerate, *J. Mol. Biol.* (2009), doi:10.1016/j.jmb.2009.09.012

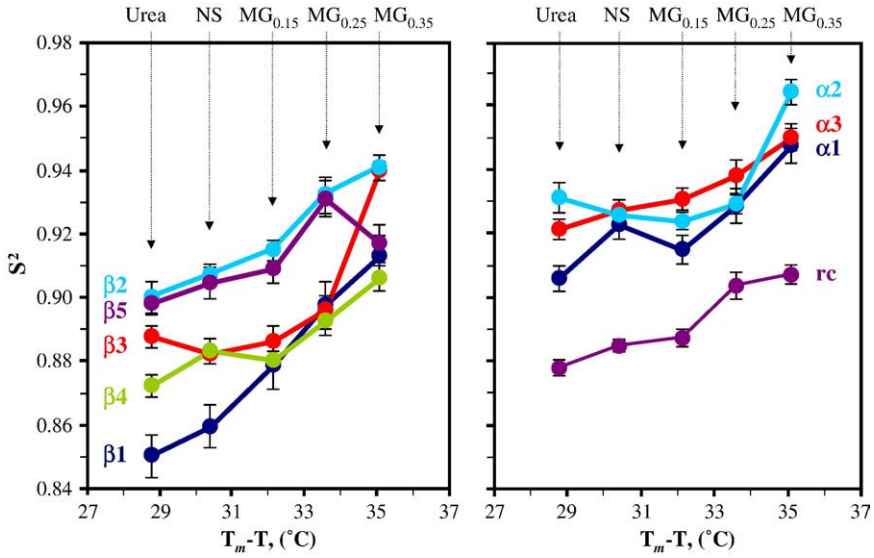

Fig. 5. Average S^2 values of the secondary structural elements of SNase as a function of the shift away from the melting temperature. The amide protons were grouped as a function of secondary structural elements, and the respective S^2 values were averaged. The different experimental conditions are specified on top of the plots. NS, no solute; MG, mannosylglycerate (subscripts indicate solute concentration in molar units).

EX2 regime holds ($k_{cl}>>k_{ch}$)[33,34] and Eq. 4 can be used to estimate the free energy of the structural opening reaction (ΔG_{HX}).

$$\text{NHclosed} \underset{k_{cl}}{\overset{k_{op}}{\leftrightarrows}} \text{NHopen} \xrightarrow{k_{ch}} \text{Exchange} \qquad (3)$$

$$\Delta G_{HX} = -RT\ln K_{op} = -RT\ln(k_{ex}/k_{ch}) \qquad (4)$$

Here, k_{ch} represents the chemical exchange rate of a freely accessible amide proton and depends on a variety of factors (pH, temperature, neighbouring side chains, and isotopic effects) that have been calibrated by Bai *et al.*[35] The k_{ex} is the experimentally observed exchange rate for a given amide proton. The ratio k_{ex}/k_{ch} is defined as the protection factor. Assuming that the solute does not change the k_{ch} significantly, and the results from the CLEANEX-PM experiments indicate that there is less than a 2-fold change, the variation of the free energy values ($\delta\Delta G_{HX}$) caused by the solute can be determined using the following equation:

$$\delta\Delta G_{HX} = -RT\ln\left(k_{ex}/k_{ex}^{solute}\right) \qquad (5)$$

At 30 °C (lowest examined temperature), the estimated free energy values for the structural opening reaction varied between 23.6 and 43.5 kJ mol^{-1}, while at 47 °C, the free energy values ranged between 21.3 and 31.6 kJ mol^{-1}. The presence of mannosylglycerate (0.25 M) caused a general increase of the ΔG_{HX} values. The values of $\delta\Delta G_{HX}$

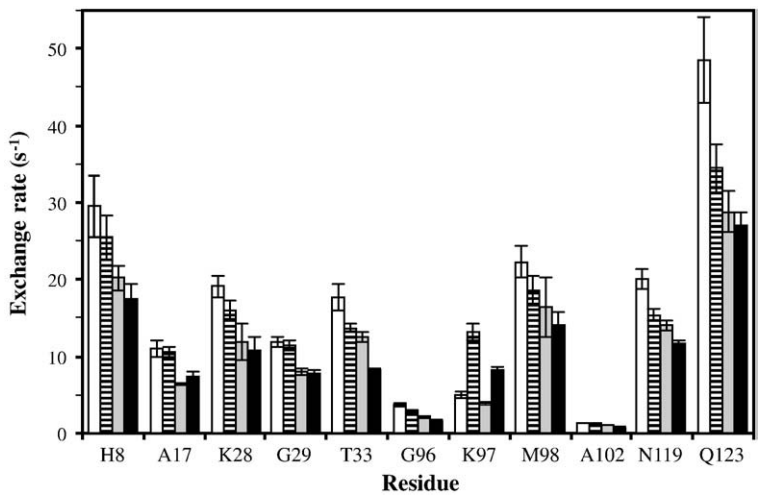

Fig. 6. Fast water–amide proton exchange rates (in s^{-1}) obtained for SNase using the CLEANEX-PM technique. The plot depicts amide protons that exchange with the solvent in the millisecond range at 37 °C and pH 7.3 (10 mM phosphate buffer). Rates were measured in the absence of solutes (open bars) and in the presence of 0.25 M KCl (striped bars), 0.60 M glycerol (grey bars), and 0.25 M mannosylglycerate (solid bars).

Please cite this article as: Pais, T. M., *et al.*, Relationship between Protein Stabilization and Protein Rigidification Induced by Mannosylglycerate, *J. Mol. Biol.* (2009), doi:10.1016/j.jmb.2009.09.012

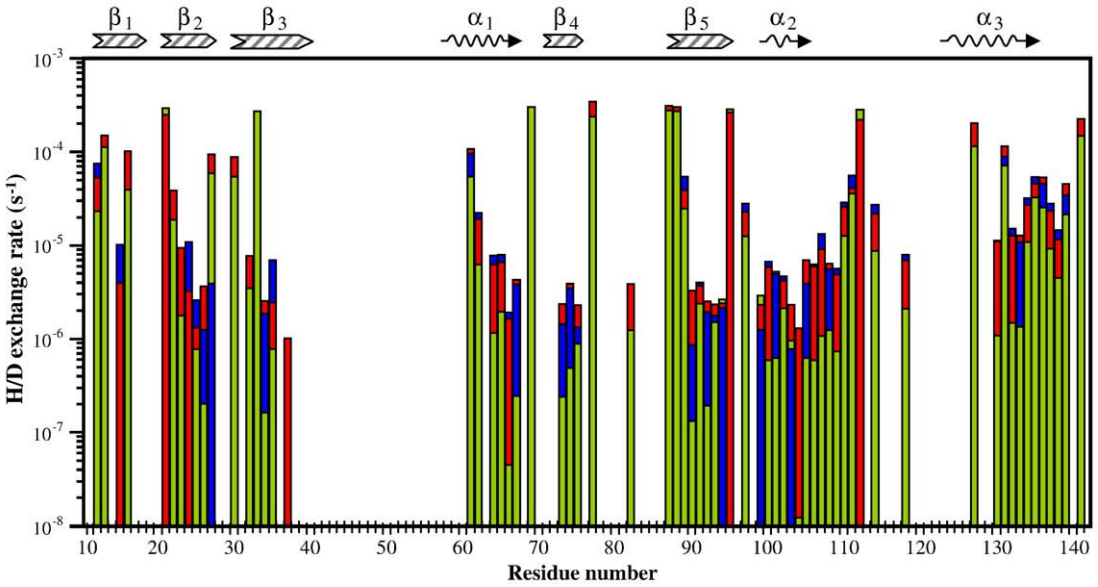

Fig. 7. Effect of mannosylglycerate on the amide hydrogen/deuterium (H/D) exchange rates. The plot illustrates the exchange rates of amide protons of SNase at 37 °C in the presence of 0.25 M of mannosylglycerate (green bars), 0.25 M of KCl (red bars), and 0.60 M glycerol (blue bars). The rates are shown on a logarithmic scale, and the horizontal axis represents the amino acid sequence. For each residue, the bars are ordered according to the magnitudes of the exchange rates, with the lowest exchange rate at the front, and overlaid. Thus, the dominant green colour shows that the lowest rates generally occur in the presence of mannosylglycerate.

(Eq. 5) obtained at 42 °C (the temperature that allowed the comparison of the largest number of ΔG_{HX} values) showed that the residues involved in α-helix 2 are significantly more stabilized than the residues in other secondary structural motifs, whereas β-strand 1 and α-helix 3, located at the N- and C-termini, respectively, were much less stabilized by mannosylglycerate (Table 4). The ΔG_{HX} values obtained from the 30 amide groups that were accessible at all studied temperatures were averaged to obtain a global ΔG_{HX} as a function of temperature (Fig. 8). This shows that mannosylglycerate has a stabilizing effect over the full temperature range.

Chemical shift variation of amide protons

The chemical shift of 97 amide protons was measured as a function of the concentration of the different solutes. Mannosylglycerate caused very small chemical shift variations, but the majority of the residues showed a linear trend as a function of solute concentration, with the chemical shifts being displaced towards higher frequencies (Supplementary Fig. S2). Fairly linear chemical shift variations were also observed with increasing amounts of the other tested solutes. This allowed the determination of an NH solute coefficient ($\Delta\delta^{sol}$), defined as the change in chemical shift with concentration (Fig. 9). The mean coefficients were 0.22±0.04 ppm M^{-1} for mannosylglycerate, 0.20±0.06 ppm M^{-1} for KCl, 0.16±0.01 ppm M^{-1} for glycerol, and −0.55± 0.03 ppm M^{-1} for urea (error values represent the SD). These values show that the chemical shift variations are not correlated with stabilization of the protein. Weak correlations (correlation coefficients $R^2<0.2$) were found between individual NH solute coefficients obtained with mannosylglycerate or KCl and parameters such as hydrogen-bond score (estimated by the WHATIF web interface),[36] relative surface exposure (accessibility of residues as if they were mutated to an alanine), or side-chain accessible molecular surface (Supplementary Fig. S3).

Mannosylglycerate had little effect on the variation of NH chemical shifts with temperature

Table 4. Added stability of SNase induced by the presence of 0.25 M mannosylglycerate as measured by the variation of proton exchange rates at 42 °C

	Average ΔG_{HX} (kJ mol^{-1})[a]		$\delta\Delta G_{HX}$ (kJ mol^{-1})	No. of residues included
	No sol	MG	MG − no sol	
β-Strand 1	24.83 (±0.17)	27.81 (±0.15)	2.98 (±0.23)	4
β-Strand 2	27.64 (±0.08)	32.30 (±0.14)	4.66 (±0.16)	6
β-Strand 3	29.75 (±0.10)	34.29 (±0.52)	4.54 (±0.53)	6
α-Helix 1	27.33 (±0.08)	32.91 (±0.17)	5.58 (±0.19)	6
β-Strand 4	27.06 (±0.04)	32.42 (±0.24)	5.36 (±0.24)	2
β-Strand 5	29.24 (±0.07)	34.54 (±0.27)	5.30 (±0.28)	6
α-Helix 2	29.53 (±0.04)	35.71 (±0.38)	6.18 (±0.38)	7
α-Helix 3	26.94 (±0.12)	30.50 (±0.07)	3.56 (±0.14)	7
Global	28.04 (±0.03)	32.70 (±0.08)	4.66 (±0.08)	59

Secondary structure elements are numbered from the N-terminus to the C-terminus in the SNase sequence.

[a] The values represent the average of all the residues in a particular secondary structural element that could be measured in the absence and in the presence of mannosylglycerate. Associated errors were estimated from the individual uncertainties of each ΔG_{HX} value using the fundamental equation of error propagation. No sol, no solute; MG, mannosylglycerate.

Please cite this article as: Pais, T. M., *et al.*, Relationship between Protein Stabilization and Protein Rigidification Induced by Mannosylglycerate, *J. Mol. Biol.* (2009), doi:10.1016/j.jmb.2009.09.012

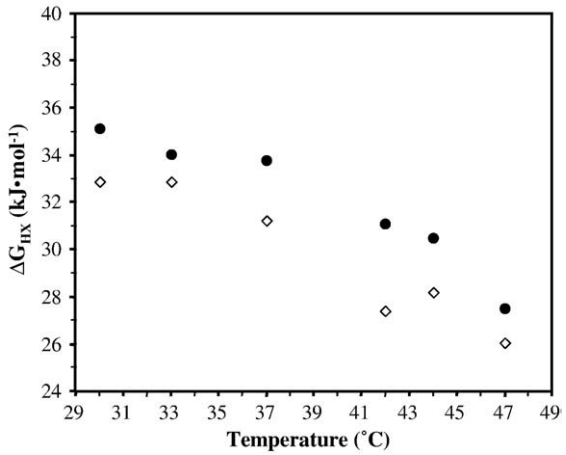

Fig. 8. Free energy of the structural opening reaction associated with hydrogen/deuterium exchange of SNase as a function of temperature with or without mannosylglycerate. The global free energy values (ΔG_{HX}) for protein unfolding were estimated by averaging the values for the 30 amide protons with exchange rates that were accessible at all the temperatures used. The error associated with the global free energy values was lower than 0.5 kJ mol^{-1}. Solid circles represent measurements with 0.25 M mannosylglycerate, and open diamonds those with 0.25 M KCl.

(Supplementary Fig. S4). The average NH temperature coefficient was found to be −3.2 ppb K^{-1} in the presence and in the absence of mannosylglycerate. This supports the notion that solutes do not have any measurable impact on the structure of the native state.

Discussion

Understanding the mechanisms for stabilization of proteins by compatible solutes is of great importance from a fundamental as well as an applied point of view.[37,38] It is generally accepted that solutes do not affect the structure of proteins in a significant way, but alterations in the pattern of protein dynamics have been reported.[15–17,39] However, the relationship between flexibility and stability remains debatable.[40,41] Studying the influence of solute concentration on protein stability has a number of advantages over studies of pairs of systems such as proteins from mesophilic and hyperthermophilic organisms, point mutants, enzymes with and without bound substrates, or oxidised and reduced centers.[20,42–44] In each of those cases, it is difficult to separate the effects of the local differences from the effects that correlate directly with protein stability. The present work allowed the dynamic properties of a single protein to be measured as its stability was varied. To ascertain whether the stabilization rendered by solutes is associated with changes in internal mobility, we performed a thorough characterisation of the effect of mannosylglycerate on the internal motions of a model protein, using different NMR experiments to access multiple times scales.

A strong correlation was observed between the stability of SNase in each of the conditions studied and the respective generalised order parameters. In particular, a linear correlation was found between S^2 values and the melting temperature at increasing concentrations of mannosylglycerate (Fig. 4). Curiously, the addition of mannosylglycerate (0.35 M at

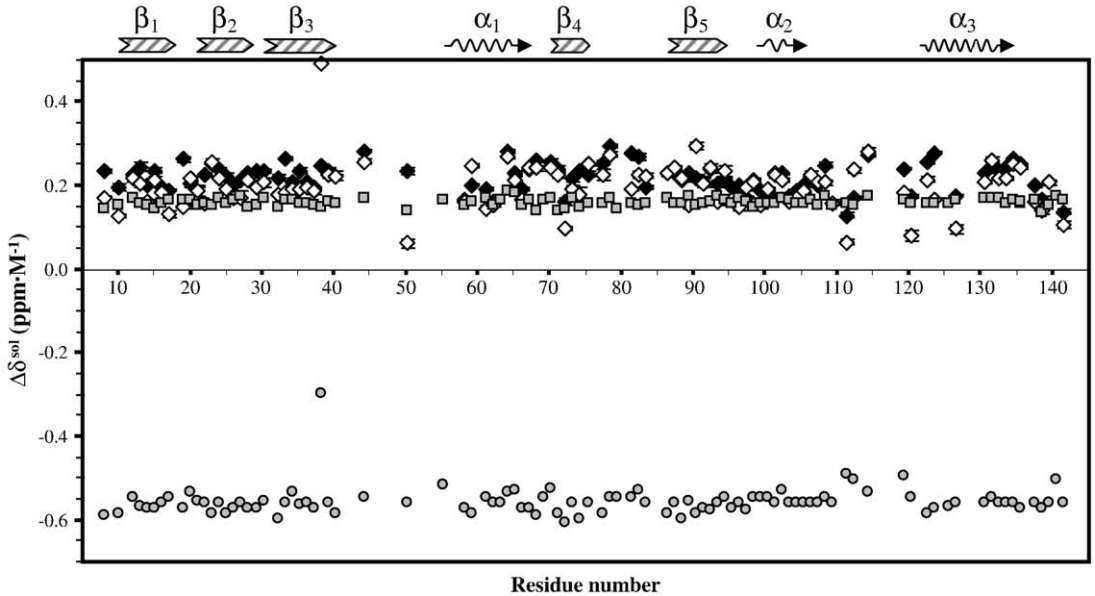

Fig. 9. Variation of the NH chemical shifts in SNase as a function of solute concentration. $\Delta\delta^{sol}$ represents the slope of the chemical shift variation for each amide proton. The values were obtained by fitting measurements made with concentrations in the range 0 to 0.25 M solute (0–0.6 M in the case of glycerol) at pH 5.1 (acetate buffer) and 37 °C and extrapolated to 1 M. Values for KCl (open diamonds), mannosylglycerate (black diamonds), glycerol (grey squares), and urea (grey circles) are expressed in ppm M^{-1}.

Please cite this article as: Pais, T. M., *et al.*, Relationship between Protein Stabilization and Protein Rigidification Induced by Mannosylglycerate, *J. Mol. Biol.* (2009), doi:10.1016/j.jmb.2009.09.012

37 °C) resulted in a restriction of the SNase fast motions comparable to that brought about by a reduction of 5 °C in the working temperature. This correlation is further strengthened by the observation that an increase in the experimental temperature, or the addition of urea, resulted in a decrease of the generalised order parameters. Interestingly, the effect of mannosylglycerate appears to be greater on residues involved in α-helices and β-strands than on less structured regions of the protein, such as loops, turns, and termini, suggesting a strengthening of intramolecular interactions in the protein.

These results suggest a link between induced protein stabilization and backbone rigidification, as the effect of mannosylglycerate on protein dynamics in the picosecond to nanosecond timescale clearly correlates with extra stability conferred by this solute. However, this does not mean that a more stable protein will necessarily be more rigid, since differences in amino acid composition may confer added stability through other mechanisms.[14] Indeed, comparison of homologous proteins from thermophilic and mesophilic origins has shown a marked reduction in picosecond to nanosecond timescale motions in the more stable proteins in some cases, but not in others.[40,42,43]

The CLEANEX-PM experiment is used to quantify water–NH exchange in the millisecond range.[31] The presence of mannosylglycerate decreased the values of all the exchange rates measurable by this technique by similar factors (a decrease of 1.5- to 2.5-fold). However, the viscosity of the solution appears to have a comparable effect, and thus it is difficult to draw conclusions about its relevance to the stabilization of SNase. As the residues in question are poorly shielded from solvent access, these small effects might be caused by the influence of the water structure in the hydration shell of the protein (i.e., a change in k_{ch}, the exchange rate for unprotected protons). A study of *Pyrococcus furiosus* rubredoxin at high pH[45] found amide proton exchange occurring throughout the structure on the millisecond timescale, despite the high stability of the native protein. Similarly, the addition of 1 M sucrose to ribonuclease A increased the stability by 5 °C[46] but had little effect on fast and intermediate exchange.[17] Thus, it seems that proton exchange on the millisecond timescale is not related to protein stability.

The most slowly exchanging amide protons are only expected to exchange with deuterium through motions that lead to partial protein unfolding. These motions are expected to be much slower and larger-scale than those characterised by the S^2 parameter. The large reduction induced by mannosylglycerate in the exchange rates of the most protected amide protons implies that the fraction of time that the protein remains in the partially unfolded state has also decreased; this means that the protein mobility has decreased in the sense that the time-averaged structure is tighter. However, the rate constants for closing and opening are not determined (Eq. 3). Exchange rates may also be affected by changes in k_{ch}, but the effects observed using CLEANEX-PM place an upper limit on this and show that it is not a major factor.

Several authors defend the existence of intermediate states in the folding pathway of SNase, proposing more or less complex models.[47,48] However, the exchange reaction for each individual proton is always described by a two-state model where the proton can only be in the closed or open state, with a constant k_{ch}, independent of the conformational state of the rest of the protein. In this sense, the closed state for a specific proton is a native-like environment for that proton, although it may not be the native state of the entire protein. Whatever the detailed mechanism of SNase folding, the exchange rates (accessible by the method employed here) that are slowed due to the presence of mannosylglycerate imply a shift in the equilibrium towards the closed state. Hence, if a generalised reduction of the amide proton exchange rates is observed, then it remains true that the time-averaged structure of the protein is more compact.

In the case of SNase, the exchange rates of the very slowly exchanging amide protons located at the center of secondary structural motifs appear to be more affected by mannosylglycerate than those located at the periphery (Supplementary Fig. S5). This points to a cumulative effect of the solute on the exchange rates of the amide protons located within a structural motif or within the same sublocal unfolding unit—the foldons.[49,50] At 42 °C, half of the measured hydrogen exchange rates (i.e., 29) were from residues involved in these foldon substructures. The presence of mannosylglycerate resulted in a reduction of the hydrogen exchange rates of more than 7-fold for 24 residues within foldons, whereas only 4 (out of 28) of the residues that were not within foldons experienced similar variations of their amide proton exchange rates. This suggests that mannosylglycerate affects primarily the concerted, wider motions of the protein backbone in the latter stages of unfolding, rather than more local and non-concerted motions. Furthermore, glycerol, which was used as a control for the effect of viscosity, had a relatively small influence on the exchange rates.

The average values of $\delta\Delta G_{HX}$ calculated for each secondary structural motif further support this concept (Table 4); the smallest variations of the free energies were found in β-strand 1 and α-helix 3, which are closest to the N- and C-termini, respectively. Structural elements further away from the termini are involved in a larger number of intramolecular interactions and exhibit larger variations of the free energy values upon solute addition. In summary, mannosylglycerate restrains protein motions at this slow timescale, especially of residues in the core of the protein, as observed by other authors with stabilizing osmolytes such as sucrose, glycine, or glycerol.[17,39,51]

Mannosylglycerate causes only small changes in NH chemical shifts (Supplementary Fig. S2), which is consistent with the view that the solute does not

Please cite this article as: Pais, T. M., *et al.*, Relationship between Protein Stabilization and Protein Rigidification Induced by Mannosylglycerate, *J. Mol. Biol.* (2009), doi:10.1016/j.jmb.2009.09.012

induce appreciable modifications of the protein structure. Nevertheless, the chemical shift variations showed a linear behaviour with respect to solute concentration. A weak correlation was found with the protein relative surface exposure and side-chain accessible molecular surface but not with backbone accessible molecular surface, suggesting that the mannosylglycerate-induced chemical shift variations occur via solute side-chain interactions. However, the evidence for mannosylglycerate binding is rather weak.

Concluding remarks

Mannosylglycerate was shown to induce restriction of the protein motions on all the timescales that were studied, but the effect on proton exchange on the millisecond timescale was weak. A strong correlation was established between restriction of the high frequency motions and the increased stability of SNase as a function of mannosylglycerate concentration, and this was not a consequence of an increase of the ionic strength or the viscosity of the solution. It should be stressed that this correlation does not imply an obligatory connection between the intrinsic stability and the rigidity of individual proteins. Actually, an increasing number of experimental data have challenged the intuitive association between highly stable proteins and high rigidity.[40,41] Further studies on the effect of stabilizing solutes on protein dynamics will be necessary to determine how general the established link between protein rigidification and stabilization is.

Materials and Methods

Protein production

The PHS variant of SNase protein includes three substitutions: P117G, H124L, and S128A. This protein is considerably more stable than the wild type.[52] The respective ribbon diagram generated with the program MOLMOL[23] is depicted in Fig. 2.

The plasmid containing the gene for PHS SNase was transformed in *Escherichia coli* BL21(DE) for overexpression. Cells were grown at 37 °C on ^{15}N-labelled defined medium[16] (or LB medium) supplemented with kanamycin. Protein overexpression was started by adding β-D-thiogalactopyranoside (1 mM final concentration) to the cell culture at an $OD_{600\ nm}$ of 0.6. The cells were harvested 5 h after the induction by low-speed centrifugation (2000*g*, 10 min). Protein purification proceeded as described elsewhere[53] with some modifications: the urea buffer was adjusted to pH 8; the protein solution was loaded onto a single column (Sepharose Fast Flow, Pharmacia Uppsala Sweden); acetone was not used for the precipitation steps; and the final dialysis was carried out first in 1 M KCl and then in distilled H_2O.

The final protein concentration was calculated by measuring the absorbance at 280 nm and using an extinction coefficient of 0.93 (cm mg ml^{-1}). Purity was above 95% as assessed by SDS-PAGE with Coomassie staining. The purified protein was flash-frozen with liquid nitrogen in small drops and stored at −80 °C.

Differential scanning calorimetry

DSC was performed on a MicroCal VP-DSC MicroCalorimeter equipped with 0.51 ml cells and controlled by the VP-viewer program (Microcal, Century City, CA). Temperature and heat flow were calibrated according to MicroCal instructions. Stock solutions were prepared by extensive dialysis of concentrated SNase against phosphate buffer (10 mM, pH 7.5). A volume of 2 ml of phosphate buffer with or without solute was prepared and divided equally into two Eppendorf tubes. An aliquot of the concentrated protein solution or an equal volume of phosphate buffer was added to each of the tubes. These solutions were then used to fill the sample and reference cells, respectively. DSC scans were run from 20 to 90 °C at a constant heating rate of 1 °C/min. Reversibility was assessed by performing two sequential DSC scans with the same protein solution. The transition temperature was determined, in each case, on the basis of three independent runs. The tested solutes were mannosylglycerate (0.15, 0.25, 0.35, and 0.50 M), glycerol (0.60 M), urea (0.25 M), and KCl (0.25 M).

NMR spectroscopy

Water–amide proton saturation transfer experiments (CLEANEX-PM) were acquired on a Bruker AVANCE^{III} 800 spectrometer (Bruker, Rheinstetten, Germany) operating at 800.33 MHz, using a 5-mm inverse detection probe with field gradients on the *z*-axis. All other NMR experiments were performed on a Bruker DRX 500 spectrometer (Bruker) at 500.13 MHz, with a broadband inverse detection 5-mm probe head with triple axis pulsed field gradients. All NMR data were collected using ^{1}H–^{15}N HSQC detection schemes. The control sample used for the NMR experiments contained uniformly ^{15}N-labelled SNase (2.6 mM) and acetate-d_4 buffer (60 mM, pH 5.1), except for the CLEANEX-PM experiments where phosphate buffer (10 mM, pH 7.3) was used instead. Other samples differ from the control by the presence of one of these solutes: mannosylglycerate (0.15, 0.25, and 0.35 M), glycerol (0.60 M), urea (0.25 M), or KCl (0.25 M). Glycerol and KCl were used to assess the contributions of viscosity and ionic strength, respectively, to the results observed with 0.25 M mannosylglycerate. The viscosity of 0.6 M glycerol is identical with that of 0.25 M mannosylglycerate. The viscosity of mannosylglycerate solutions was determined using an Ubbelohde type viscometer.

The assignment of the resonances present in the HSQC spectrum was performed by comparison with previously published data on the SNase structure.[18,19] The resonances corresponding to the mutated residues were not assigned, since NMR information was not available at the time of this study.

^{15}N relaxation measurements and analysis

^{15}N relaxation rates were measured for the amide groups of SNase at 37 °C in the absence (control) and in the presence of four solutes: mannosylglycerate (0.15, 0.25, and 0.35 M), urea (0.25 M), glycerol (0.60 M), and KCl (0.25 M). Studies with higher concentrations of mannosylglycerate were hampered by severe line broadening. Two additional sets of relaxation measurements were carried out for the control sample (no solutes) at 32 and 42 °C. Longitudinal (T_1) and transverse (T_2) relaxation times and ^{1}H–^{15}N steady-state heteronuclear

Please cite this article as: Pais, T. M., *et al.*, Relationship between Protein Stabilization and Protein Rigidification Induced by Mannosylglycerate, *J. Mol. Biol.* (2009), doi:10.1016/j.jmb.2009.09.012

NOE (h-NOE) values were measured using conventional sequences[54] with some modifications regarding water suppression. For T_1 measurements, a 3-9-19 WATERGATE sequence was used,[55] while in the case of T_2, water suppression was achieved by a WATERGATE sequence with selective inversion of the water signal. In the h-NOE experiment without proton saturation, water suppression was achieved by selective inversion of the water resonance and by the use of gradient pulses to select for the $^{15}N \rightarrow {}^{1}H$ coherence transfer pathway.

T_1 relaxation rates (R_1) were obtained with relaxation periods of 0, 20, 50, 100, 250, 500, 1000, 1250, and 1500 ms. Values for the T_2 relaxation rates (R_2) were obtained with a Carr–Purcell–Meiboom–Gill spin-echo period of 500 μs and relaxation periods of 0, 16, 32, 48, 56, 64, 96, and 144 ms. In order to measure h-NOEs, spectra acquired with and without saturation of protons were recorded in an interleaved manner to minimize systematic differences. ^{1}H saturation was achieved by the application of 120° pulses spaced at 5-ms intervals for 3 s.[56] The total recycling delay for both experiments was 4.2 s.

The number of scans accumulated per t_1 increment for the T_1, T_2, and h-NOE experiments was 24, 32, and 36 scans, respectively. The peak intensities were measured using XWinNMR software (Bruker). The h-NOE values were calculated using the ratio between the volume of each $^{1}H–^{15}N$ correlation peak in the presence or absence of proton saturation. Relaxation rates for T_1 and T_2 were determined by nonlinear least-squares fitting of the peak volumes to a mono-exponential decay function. Error estimates were obtained from the SD of the fitting coefficients.

The Tensor2 program[22,24] was used to characterise the diffusion tensor of the SNase by analysing the R_2/R_1 ratios obtained for each of the examined conditions. Residues with significant internal motion or in fast chemical exchange were excluded from the characterisation of the diffusion properties of the protein.[21] Error estimates were obtained from 600 Monte Carlo simulations, while χ^2 and *F*-test analyses were used to evaluate the quality of the fit and the statistical significance of introducing an extra parameter to the diffusion model (isotropic, axial, or fully anisotropic diffusion). The same program was used to select the dynamic model that best described the internal mobility of the protein backbone based on the relaxation data collected. This software uses the Lipari–Szabo type analysis.[57,58] The analysis was performed using an average amide bond length of 1.02 Å and a chemical shift anisotropy value approximated to −170 ppm for ^{15}N nuclei.[59]

Five increasingly complex models were tested iteratively as described by Mandel *et al.*[25] optimizing the parameters S^2, τ_e, R_{ex}, S^2_f, and S^2_s, where S^2 is the generalised order parameter characterising the amplitude of the internal motions, τ_e is the effective correlation time for the internal motions, R_{ex} is the exchange contribution to T_2, and subscripts "f" and "s" indicate fast and slow timescale motions, respectively.

Model selection was done automatically by the program Tensor2, and error estimates were obtained by 600 Monte Carlo simulations. This procedure was repeated with the data collected from all the other conditions at which ^{15}N relaxation experiments were performed.

Water–amide proton saturation transfer experiments

Water–amide proton exchange rates in the millisecond range were measured by saturation transfer spectroscopy using the phase-modulated CLEAN chemical exchange technique (CLEANEX-PM) with a fast-HSQC detection scheme.[26,31,60] This technique has been shown to suppress NOE contributions from other protons with chemical shifts coincident with water (e.g., $C^{\alpha}H$) as well as contributions from exchange-relayed NOEs of rapidly exchanging protons. Thus, it was possible to measure pure exchange rates for the observed amide groups. The experiments were performed at 37 °C on a Bruker AVANCE^{III} 800 spectrometer. Four samples of SNase were prepared in 10 mM phosphate buffer (pH 7.3) without solutes or with one of the following additives: mannosylglycerate (0.25 M), KCl (0.25 M), and glycerol (0.60 M). As stated already, glycerol and KCl were used as controls for the viscosity and ionic strength of mannosylglycerate (0.25 M), respectively.

The CLEANEX-PM experiments were collected with mixing times of 5, 8, 10, 15, 20, and 35 ms with repetition of the 20-ms mixing time experiment to estimate the SD of peak volumes. These spectra were acquired with 2048 complex data points, 256 time increments, and 8 scans per increment. A delay of 3 s was used between scans to minimize the level of water saturation.

Additional NMR experiments were necessary to quantify water–amide exchange rates accurately.[31] These included (i) fast-HSQC spectra for determination of reference peak volumes, (ii) measurements of water saturation level in the CLEANEX-PM sequence, and (iii) inversion recovery spectra for water T_1 determination, according to the method described by Hwang *et al.*[26]

Proton/deuterium exchange rates

Proton/deuterium exchange experiments were performed to monitor exchange rates of slowly exchanging amide protons (minute to hour timescale), using protein samples with KCl (0.25 M), mannosylglycerate (0.25 M), or glycerol (0.60 M). Exchange rates were measured for the protein samples at six temperatures: 30, 33, 37, 42, 44, and 47 °C. Glycerol-containing samples were only examined at 37 °C. The proton/deuterium exchange reaction was initiated by dissolving the lyophilised protein samples in 99.9% $^{2}H_2O$. The resulting pH of 5.7 was measured with a glass electrode without further corrections.

The exchange rates were determined by measuring the volume of amide cross-peaks in HSQC spectra as a function of time. Spectra were acquired with 2048 complex data points, 256 time increments, and 8 scans per increment. All experiments started less than 25 min after the exchange reaction was initiated. Standard Bruker pulse sequences were used to collect HSQC spectra with sensitivity enhancement. The peak volumes were measured with XWinNMR software (Bruker) and fitted to a first-order decay curve by nonlinear regression, providing the exchange rate for each amide proton.

Amide proton chemical shift variation

Chemical shift variation as a function of solute concentration was followed at 37 °C by $^{1}H–^{15}N$ HSQC spectra with the same acquisition parameters as in the hydrogen/deuterium exchange experiments. Increasing amounts of KCl or mannosylglycerate (up to 0.25 M final concentration) were added to an initial control sample (no solutes) and HSQC spectra were recorded for each condition. Protein samples containing either 0.25 M urea or 0.60 M glycerol were also examined by $^{1}H–^{15}N$ HSQC spectra.

The temperature dependence of amide proton chemical shifts was also evaluated for SNase samples in the absence

Please cite this article as: Pais, T. M., *et al.*, Relationship between Protein Stabilization and Protein Rigidification Induced by Mannosylglycerate, *J. Mol. Biol.* (2009), doi:10.1016/j.jmb.2009.09.012

of solutes and in the presence of 0.35 M mannosylglycerate. A temperature range of 22 degrees (27– 49 °C) was used to determine the amide proton temperature coefficients of all accessible resonances. The chemical shifts were measured using the TOPSPIN 2.0 software (Bruker) and referenced to dioxane in a capillary.

Acknowledgements

This work was supported by Fundação para a Ciência e a Tecnologia (FCT), Portugal, Projects POCI/BIA-PRO/57263/2004 and PTDC/BIO/70806/2006. The authors acknowledge Dr. Tiago Faria, ITQB, for valuable help with the statistics analysis and protein production. T.M.P. acknowledges FCT for grant support (SFRH/BD/42210/2007). The NMR spectrometers are part of the National NMR Network and were acquired with funds from FCT and FEDER.

Supplementary Data

Supplementary data associated with this article can be found, in the online version, at doi:10.1016/j.jmb.2009.09.012

References

1. Nozaki, Y. & Tanford, C. (1963). The solubility of amino acids and related compounds in aqueous urea solutions. *J. Biol. Chem.* **238**, 4074–4081.
2. Nozaki, Y. & Tanford, C. (1965). The solubility of amino acids and related compounds in aqueous ethylene glycol solutions. *J. Biol. Chem.* **240**, 3568–3575.
3. Nozaki, Y. & Tanford, C. (1970). The solubility of amino acids, diglycine, and triglycine in aqueous guanidine hydrochloride solutions. *J. Biol. Chem.* **245**, 1648–1652.
4. Arakawa, T. & Timasheff, S. N. (1985). The stabilization of proteins by osmolytes. *Biophys. J.* **47**, 411–414.
5. Timasheff, S. N. (1992). Water as ligand: preferential binding and exclusion of denaturants in protein unfolding. *Biochemistry*, **31**, 9857–9864.
6. Timasheff, S. N. (1993). The control of protein stability and association by weak interactions with water: how do solvents affect these processes? *Annu. Rev. Biophys. Biomol. Struct.* **22**, 67–97.
7. Liu, Y. & Bolen, D. W. (1995). The peptide backbone plays a dominant role in protein stabilization by naturally occurring osmolytes. *Biochemistry*, **34**, 12884–12891.
8. Auton, M. & Bolen, D. W. (2004). Additive transfer free energies of the peptide backbone unit that are independent of the model compound and the choice of concentration scale. *Biochemistry*, **43**, 1329–1342.
9. Auton, M., Holthauzen, L. M. & Bolen, D. W. (2007). Anatomy of energetic changes accompanying urea-induced protein denaturation. *Proc. Natl Acad. Sci. USA*, **104**, 15317–15322.
10. Santos, H., Lamosa, P., Faria, T. Q., Borges, N. & Neves, C. (2007). The physiological role, biosynthesis and mode of action of compatible solutes from (hyper) thermophiles. In *Physiology and biochemistry of extremophiles* (Gerday, C. & Glandorf, N., eds), pp. 86–103.
11. Faria, T. Q., Mingote, A., Siopa, F., Ventura, R., Maycock, C. & Santos, H. (2008). Design of new enzyme stabilizers inspired by glycosides of hyperthermophilic microorganisms. *Carbohydr. Res.* **343**, 3025–3033.
12. Pais, T. M., Lamosa, P., dos Santos, W., LeGall, J., Turner, D. L. & Santos, H. (2005). Structural determinants of protein stabilization by solutes. The importance of the hairpin loop in rubredoxins. *FEBS J.* **272**, 999–1011.
13. Razvi, A. & Scholtz, J. M. (2006). Lessons in stability from thermophilic proteins. *Protein Sci.* **15**, 1569–1578.
14. Petsko, G. A. (2001). Structural basis of thermostability in hyperthermophilic proteins, or "there's more than one way to skin a cat". *Methods Enzymol.* **334**, 469–478.
15. Doan-Nguyen, V. & Loria, J. P. (2007). The effects of cosolutes on protein dynamics: the reversal of denaturant-induced protein fluctuations by trimethylamine *N*-oxide. *Protein Sci.* **16**, 20–29.
16. Lamosa, P., Turner, D. L., Ventura, R., Maycock, C. & Santos, H. (2003). Protein stabilization by compatible solutes. Effect of diglycerol phosphate on the dynamics of *Desulfovibrio gigas* rubredoxin studied by NMR. *Eur. J. Biochem.* **270**, 4606–4614.
17. Wang, A., Robertson, A. D. & Bolen, D. W. (1995). Effects of a naturally occurring compatible osmolyte on the internal dynamics of ribonuclease A. *Biochemistry*, **34**, 15096–15104.
18. Wang, J. F., Mooberry, E. S., Walkenhorst, W. F. & Markley, J. L. (1992). Solution studies of staphylococcal nuclease H124L. 1. Backbone ^{1}H and ^{15}N resonances and secondary structure of the unligated enzyme as identified by three-dimensional NMR spectroscopy. *Biochemistry*, **31**, 911–920.
19. Wang, J. F., Hinck, A. P., Loh, S. N., LeMaster, D. M. & Markley, J. L. (1992). Solution studies of staphylococcal nuclease H124L. 2. ^{1}H, ^{13}C, and ^{15}N chemical shift assignments for the unligated enzyme and analysis of chemical shift changes that accompany formation of the nuclease-thymidine 3′,5′-bisphosphate-calcium ternary complex. *Biochemistry*, **31**, 921–936.
20. Alexandrescu, A. T., Jahnke, W., Wiltscheck, R. & Blommers, M. J. (1996). Accretion of structure in staphylococcal nuclease: an ^{15}N NMR relaxation study. *J. Mol. Biol.* **260**, 570–587.
21. Tjandra, N., Kuboniwa, H., Ren, H. & Bax, A. (1995). Rotational dynamics of calcium-free calmodulin studied by ^{15}N-NMR relaxation measurements. *Eur. J. Biochem.* **230**, 1014–1024.
22. Dosset, P., Hus, J. C., Blackledge, M. & Marion, D. (2000). Efficient analysis of macromolecular rotational diffusion from heteronuclear relaxation data. *J. Biomol. NMR*, **16**, 23–28.
23. Koradi, R., Billeter, M. & Wuthrich, K. (1996). MOLMOL: a program for display and analysis of macromolecular structures. *J. Mol. Graph.* **14**, 32–51.
24. Cordier, F., Caffrey, M., Brutscher, B., Cusanovich, M. A., Marion, D. & Blackledge, M. (1998). Solution structure, rotational diffusion anisotropy and local backbone dynamics of *Rhodobacter capsulatus* cytochrome c_2. *J. Mol. Biol.* **281**, 341–361.
25. Mandel, A. M., Akke, M. & Palmer, A. G., III (1995). Backbone dynamics of *Escherichia coli* ribonuclease HI: correlations with structure and function in an active enzyme. *J. Mol. Biol.* **246**, 144–163.
26. Hwang, T. L., Mori, S., Shaka, A. J. & van Zijl, P. C. (1997). Application of phase-modulated CLEAN

Please cite this article as: Pais, T. M., *et al.*, Relationship between Protein Stabilization and Protein Rigidification Induced by Mannosylglycerate, *J. Mol. Biol.* (2009), doi:10.1016/j.jmb.2009.09.012

chemical EXchange spectroscopy (CLEANEX-PM) to detect water–protein proton exchange and intermolecular NOEs. *J. Am. Chem. Soc.* **119**, 6203–6204.
27. Jeener, J., Meier, B. H., Bachmann, P. & Ernst, R. R. (1979). Investigation of exchange processes by two-dimensional NMR spectroscopy. *J. Chem. Phys.* **71**, 4546–4553.
28. Schwartz, A. L. & Cutnell, J. D. (1983). One- and two-dimensional NMR studies of exchanging amide protons in glutathione. *J. Magn. Reson.* **53**, 398–411.
29. Dobson, C. M., Lian, L.-Y., Redfield, C. & Topping, K. D. (1986). Measurement of hydrogen exchange rates using 2D NMR spectroscopy. *J. Magn. Reson.* **69**, 201–209.
30. Mori, S., Abeygunawardana, C., van Zijl, P. C. & Berg, J. M. (1996). Water exchange filter with improved sensitivity (WEX II) to study solvent-exchangeable protons. Application to the consensus zinc finger peptide CP-1. *J. Magn. Reson., Ser. B*, **110**, 96–101.
31. Hwang, T. L., van Zijl, P. C. & Mori, S. (1998). Accurate quantitation of water–amide proton exchange rates using the phase-modulated CLEAN chemical EXchange (CLEANEX-PM) approach with a fast-HSQC (FHSQC) detection scheme. *J. Biomol. NMR*, **11**, 221–226.
32. Englander, S. W. & Mayne, L. (1992). Protein folding studied using hydrogen-exchange labeling and two-dimensional NMR. *Annu. Rev. Biophys. Biomol. Struct.* **21**, 243–265.
33. Hvidt, A. & Nielsen, S. O. (1966). Hydrogen exchange in proteins. *Adv. Protein Chem.* **21**, 287–386.
34. Englander, S. W., Sosnick, T. R., Englander, J. J. & Mayne, L. (1996). Mechanisms and uses of hydrogen exchange. *Curr. Opin. Struct. Biol.* **6**, 18–23.
35. Bai, Y., Milne, J. S., Mayne, L. & Englander, S. W. (1993). Primary structure effects on peptide group hydrogen exchange. *Proteins*, **17**, 75–86.
36. Rodriguez, R., Chinea, G., Lopez, N., Pons, T. & Vriend, G. (1998). Homology modeling, model and software evaluation: three related resources. *Bioinformatics*, **14**, 523–528.
37. Cohen, F. E. & Kelly, J. W. (2003). Therapeutic approaches to protein-misfolding diseases. *Nature*, **426**, 905–909.
38. Davis-Searles, P. R., Saunders, A. J., Erie, D. A., Winzor, D. J. & Pielak, G. J. (2001). Interpreting the effects of small uncharged solutes on protein-folding equilibria. *Annu. Rev. Biophys. Biomol. Struct.* **30**, 271–306.
39. Foord, R. L. & Leatherbarrow, R. J. (1998). Effect of osmolytes on the exchange rates of backbone amide protons in proteins. *Biochemistry*, **37**, 2969–2978.
40. LeMaster, D. M., Tang, J., Paredes, D. I. & Hernandez, G. (2005). Enhanced thermal stability achieved without increased conformational rigidity at physiological temperatures: spatial propagation of differential flexibility in rubredoxin hybrids. *Proteins*, **61**, 608–616.
41. Kamerzell, T. J. & Middaugh, C. R. (2008). The complex inter-relationships between protein flexibility and stability. *J. Pharm. Sci.* **97**, 3494–3517.
42. Krishnamurthy, H., Munro, K., Yan, H. & Vieille, C. (2009). Dynamics in *Thermotoga neapolitana* adenylate kinase: ^{15}N relaxation and hydrogen–deuterium exchange studies of a hyperthermophilic enzyme highly active at 30 °C. *Biochemistry*, **48**, 2723–2739.
43. Butterwick, J. A., Patrick, L. J., Astrof, N. S., Kroenke, C. D., Cole, R., Rance, M. & Palmer, A. G., III (2004). Multiple time scale backbone dynamics of homologous thermophilic and mesophilic ribonuclease HI enzymes. *J. Mol. Biol.* **339**, 855–871.
44. Horne, J., d'Auvergne, E. J., Coles, M., Velkov, T., Chin, Y., Charman, W. N. *et al.* (2007). Probing the flexibility of the DsbA oxidoreductase from *Vibrio cholerae*—a ^{15}N–^{1}H heteronuclear NMR relaxation analysis of oxidized and reduced forms of DsbA. *J. Mol. Biol.* **371**, 703–716.
45. Hernandez, G., Jenney, F. E., Jr., Adams, M. W. & LeMaster, D. M. (2000). Millisecond time scale conformational flexibility in a hyperthermophile protein at ambient temperature. *Proc. Natl Acad. Sci. USA*, **97**, 3166–3170.
46. Liu, Y. & Sturtevant, J. M. (1996). The observed change in heat capacity accompanying the thermal unfolding of proteins depends on the composition of the solution and on the method employed to change the temperature of unfolding. *Biochemistry*, **35**, 3059–3062.
47. Jacobs, M. D. & Fox, R. O. (1994). Staphylococcal nuclease folding intermediate characterized by hydrogen exchange and NMR spectroscopy. *Proc. Natl Acad. Sci. USA*, **91**, 449–453.
48. Bédard, S., Krishna, M. M. G., Mayne, L. & Englander, S. W. (2008). Protein folding: independent unrelated pathways or predetermined pathway with optional errors. *Proc. Natl Acad. Sci. USA*, **105**, 7182–7187.
49. Englander, S. W., Mayne, L., Bai, Y. & Sosnick, T. R. (1997). Hydrogen exchange: the modern legacy of Linderstrom-Lang. *Protein Sci.* **6**, 1101–1109.
50. Bédard, S., Mayne, L. C., Peterson, R. W., Wand, A. J. & Englander, S. W. (2008). The foldon substructure of staphylococcal nuclease. *J. Mol. Biol.* **376**, 1142–1154.
51. Calhoun, D. B. & Englander, S. W. (1985). Internal protein motions, concentrated glycerol, and hydrogen exchange studied in myoglobin. *Biochemistry*, **24**, 2095–2100.
52. Chen, J., Lu, Z., Sakon, J. & Stites, W. E. (2000). Increasing the thermostability of staphylococcal nuclease: implications for the origin of protein thermostability. *J. Mol. Biol.* **303**, 125–130.
53. Shortle, D. & Meeker, A. K. (1989). Residual structure in large fragments of staphylococcal nuclease: effects of amino acid substitutions. *Biochemistry*, **28**, 936–944.
54. Kay, L. E., Torchia, D. A. & Bax, A. (1989). Backbone dynamics of proteins as studied by ^{15}N inverse detected heteronuclear NMR spectroscopy: application to staphylococcal nuclease. *Biochemistry*, **28**, 8972–8979.
55. Piotto, M., Saudek, V. & Sklenar, V. (1992). Gradient-tailored excitation for single-quantum NMR spectroscopy of aqueous solutions. *J. Biomol. NMR*, **2**, 661–665.
56. Markley, J. L., Horsley, W. J. & Klein, M. P. (1971). Spin-lattice relaxation measurements in slowly relaxing complex spectra. *J. Chem. Phys.* **55**, 3604–3605.
57. Lipari, G. & Szabo, A. (1982). Model-free approach to the interpretation of nuclear magnetic resonance relaxation in macromolecules 1. Theory and range validity. *J. Am. Chem. Soc.* **104**, 4546–4559.
58. Lipari, G. & Szabo, A. (1982). Model-free approach to the interpretation of nuclear magnetic resonance relaxation in macromolecules 2. Analysis of experimental results. *J. Am. Chem. Soc.* **104**, 4559–4570.
59. Tjandra, N., Wingfield, P., Stahl, S. & Bax, A. (1996). Anisotropic rotational diffusion of perdeuterated HIV protease from ^{15}N NMR relaxation measurements at two magnetic fields. *J. Biomol. NMR*, **8**, 273–284.
60. Mori, S., Wardana, C. A., Johnson, M. O. & van Zijl, P. C. (1995). Improved sensitivity of HSQC spectra of exchanging protons at short interscan delays using a new Fast-HSQC (FHSQC) detection scheme that avoids water saturation. *J. Magn. Reson., Ser B*, **108**, 94–95.

Please cite this article as: Pais, T. M., *et al.*, Relationship between Protein Stabilization and Protein Rigidification Induced by Mannosylglycerate, *J. Mol. Biol.* (2009), doi:10.1016/j.jmb.2009.09.012